Rheological Study of Highly Thixotropic Hydrogels for 3D Bio-Printing Processes

Abstract ID: 969113

Slesha Tuladhar, Cartwright Nelson, Ahasan Habib*, Sustainable Product Design and Architecture Department, Keene State College, Keene, NH 03435, USA.

Abstract

The promising success of 3D printing technique with synthetic polymers like nylon, ABS, PLA and epoxy motivates the researchers to put efforts into fabricating constructs with biocompatible natural polymers. The efforts have been broadened into various fields such as bioengineering, manufacturing, and regenerative medicine. Additive biomanufacturing commonly known as 3D bioprinting shows a lot of potential in tissue engineering with those natural polymers. Some challenges such as achieving printability, maintaining geometry in post printing stage, comforting encapsulated cells, and ensuring high proliferation are to be resolved to turn this process into a successful trial. Appropriate design of experiments with a detail rheological investigation can identify useful mechanical properties which is directly related to shape fidelity of 3D bio-printed scaffolds. As candidate natural polymers, Alginate-low viscous Carboxymethyl Cellulose (CMC) was used restricting the solid content 8% (w/v). Various rheological tests, such as the Steady Rate Sweep Test, Thixotropic (3ITT), Amplitude, and Frequency test were performed. The result indicated that rheological properties are CMC dependent. Printability and shape fidelity were analyzed of the filaments and scaffolds fabricated with all the combinations. The rheological results were co-related with the printability and shape fidelity result.

Keywords

3D bioprinting, rheology, thixotropic, printability, and Carboxymethyl cellulose.

1. Introduction

3D bio-printing is an emerging cell encapsulated biomaterial i.e. bio-ink depositing technique that uses a computer-controlled 3D printer to extrude material in a layer-upon-layer fashion [1, 2]. Due to its inherent controllability, bio-ink can be deposited in specific location to achieve the defined geometry and porosity of the fabricated scaffolds. Extrusion-based bio-printing allows among various existing 3D bio-printing techniques the usage of a diverse range of materials and compositions including heterogeneous bio-ink [3]. Hydrogels are demanding candidates for bio-printing because of its bio-compatibility and capacity to arrange 3D environment with a high water content [4].

Flowability through a small nozzle orifice and resisting deformation after releasing hydrogel from the nozzle [5] are important to have a successful extrusion process. By developing enough yield strength through quick gelation, immediate deformation after the release of the material with low viscosity can be restricted. Some factors such as by adding a viscosity modifier [6, 7], changing temperature [8], using an external cross-linker [9, 10], and controlling intrinsic rheological properties of the hydrogels [11], the rate of gelation can be controlled. Normally, in extrusionbased bio-printing, the material is cross-linked after deposition depending on the charges of the scaffold material [12]. Fabricating 3D structure with hydrogel materials ensuring the defined spatiality is challenging [12]. To facilitate this, various hydrogel materials are mixed to prepare a hybrid hydrogel [13]. Mixing of multiple hydrogel materials also helps to achieve the required rheological properties to maintain the filament geometry and eventually the scaffold geometry i.e., the shape fidelity. To achieve the required mechanical strength, one of the rheological properties such as viscosity of the hydrogel materials plays an important role [14, 15]. It becomes a conflicting choice when a hydrogel needs to create a suitable habitat for encapsulated cells during extrusion, and it needs to be high-viscous to maintain the post-printing shape fidelity [16]. Hydrogel precursors having less viscosity such as less than 300 centipoise (cps) limits the mechanically stable structure [17]. On the other hand, increasing the viscosity of the hydrogel (< 100000 cps) reduces the cell viability and proliferation but increases the mechanical integrity [18]. Sometimes viscosity is interchangeably used as the rheological properties of hydrogel materials, however, it solely cannot represent the complex rheological behavior of hydrogel materials [19, 20]. In addition to viscosity, two dynamic moduli such as storage modulus (G') and loss modulus (G") are critical [20]. Storage modulus (G') and loss modulus (G") indicate

the solid-like and liquid-like characteristics of the hydrogel material, respectively. The gelation (G'=G") point and the viscosity information can help identify the appropriate bio-ink ingredients. To ensure the shape fidelity of the fabricated scaffold at post-printing stage, identifying the recovery rate of the released hydrogel is important [21].

CMC is a water-soluble polysaccharide used for thickener or viscosity modifier. It has been reported that addition of CMC's matrix protein can help migrate and attach cell [23]. It has also been used for various drug delivery experiments [24]. In our earlier work, the effect of high viscous CMC was analyzed in bio-printing process [22]. However, to our best knowledge, the effect of low viscous CMC on bio-printing process is not reported. In this paper, we will prepare a hybrid hydrogel mixing carboxymethyl cellulose (lower molecular weight) with low viscosity at different weight percentages with alginate maintaining a constant total solid content 8% (w/v) limiting the viscosity range to 300-100000 cps. A set of rheological tests enlisted in Table 1 (b) will be conducted to determine the effect of viscosity modifier on the rheological behavior. Then, the effect of rheological behavior on the printability of the hydrogel materials will be analyzed. Finally, the effect of rheological behavior will be analyzed to determine the shape fidelity of the fabricated scaffold.

Table 1: (a) Various Composition prepared with different weight percentages of alginate and CMC and (b) An overview of all rheological tests.

Sample	Alginate	CMC	Alginate/	Rheological tests	Variables		Outcome
Sumpre	(A) (g)	(C) (g)	CMC (%)	Steady rate sweep			Flow curve, viscosity, shear
A_0C_8	0	8	0/100		(s-1)		stress, shear-thinning behavior
A_2C_6	2	6	25/75	Amplitude sweep	G1		Storage modulus (G') and loss
A_4C_4	4	4	50/50]	Shear	0.1 to 100	modulus (G"), loss tangent
A_6C_2	6	2	75/25	i İ	strain (%)	011 10 100	$(\tan \delta)$
A_8C_0	8	0	100/0	3iTT	Time	0-60/1	Recovery rate of the hydrogel
	(a)			 	(s)/Shear	61-65/100	
				į	rate (s-1)	66-185/1	(b

2. Hybrid hydrogel preparation

Alginate (alginic acid sodium salt from brown algae) and low viscous carboxymethyl cellulose (CMC) (pH: 6.80) (Sigma-Aldrich, St. Louis, MO, USA) were used as biomaterials to prepare the bio-ink. The chemical formula of those biomaterials is shown in Figure 1. Alginate is a common biopolymer, composed of (1-4)-linked β -Dmannuronic (M) and α -Lguluronic acids (G). Alginate is a negatively charged linear copolymer (M and G blocks) which is soluble in the water and supports cell growth and exhibits high biocompatibility. The G-block of this material creates bonds to form gels and GM and M blocks increase the flexibility. Carboxymethylcellulose (CMC) is another naturally or chemically derived anionic water-soluble biopolymer. CMC is a copolymer of β -D-glucose and β -D-glucopyranose-2-O-(carboxymethyl)-mono-sodium salt which are connected via β -1,4-glucosidic bonds [25]. This material is widely used as thickener [26] which is also non-toxic and non-allergenic in nature. Each glucose monomer has three hydroxyl groups which can be substituted by a carboxyl group. More substitution of the hydroxyl group by a carboxyl group makes the cellulose more soluble, thicken and stable [25]. Various weight percentages of alginate and CMC are used to prepare five different hybrid hydrogel samples (three replicates of each composition) maintaining the total solid content 8% (w/v) shown in Table 1(a). Food colors are used to differential the compositions. The overall preparation procedure of hybrid hydrogel is shown in Figure 1.

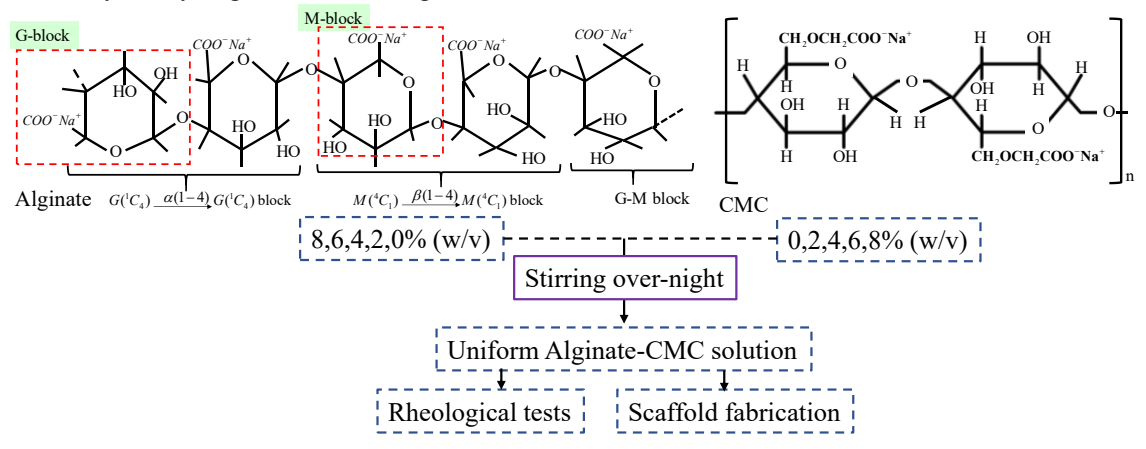


Figure 1: Preparation of hybrid hydrogel.

3. Rheological tests

Rheological measurements were performed using a rotational rheometer (MCR 102, Anton Paar, Graz, Austria) with parallel plate geometry (25.0 mm flat plate). All measurements were recorded with a 1.0 mm plate-plate gap width at room temperature (25°C). We conducted the rheological measurement at room temperature because our extrusion process was performed at room temperature which also facilitated the quick gelation of the deposited filament [16]. A set of rheological tests such as steady rate sweep test, amplitude test, and three-point interval thixotropic test were done. An overview of those tests is shown Table 1(b).

3.1. Shear thinning behavior

Shear-thinning behavior i.e. reduction of the viscosity with increasing the shear strain rate on hydrogels is crucial for extruding material through a micron-level nozzle [27]. Hydrogel with higher viscosity experiences higher shear stress during extrusion through a nozzle, which adversely affects the encapsulated cell. Therefore, shear thinning behavior of the hydrogel can help create a protective environment for encapsulated cell in extrusion-based 3D bioprinting technique.

Figure 2(a) shows the log-log plot of viscosity and shear stress vs shear strain rate respectively. Viscosity decreases with increasing the shear rate for all considered compositions. This phenomenon demonstrates the shear thinning behavior. Pure 8% alginate shows the lowest viscosity. The viscosity increases with increasing the percentage of CMC into the composition. However, at shear strain rate of 1.0 s⁻¹, A₂C₆ shows the highest viscosity. This composition may create the highest number of hydrogen and polar bond due to more easily accessible bond sites of polar carbonyl groups ($C^{\delta+} = O^{\delta-}$) which drives toward a high rate of cross-linking.

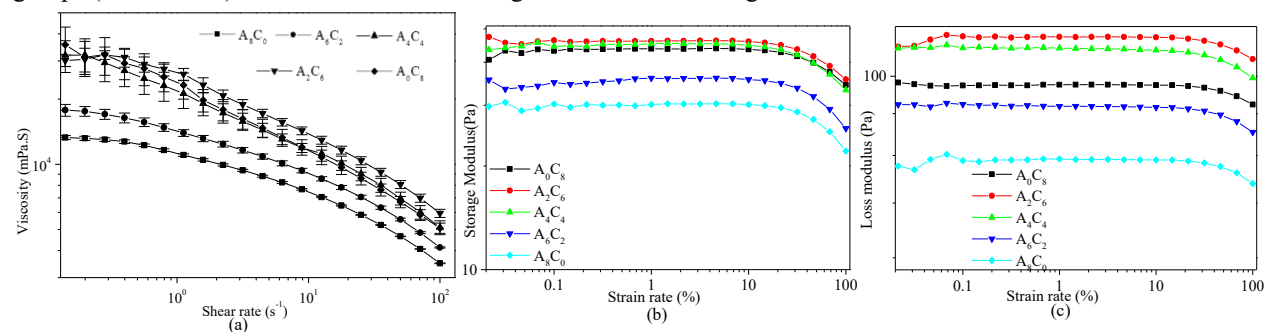


Figure 2: (a) Shear thinning behavior, (b) Storage modulus, and (c) Loss modulus.

3.2. Storage modulus and loss modulus

Complex shear modulus (G*) is one of the factors for viscoelastic suspension, is expressed by the following equation: $G^* = G' + iG'' \tag{1}$

Where, G' is the elastic (or storage) modulus, the real component and G'' viscous (or loss) modulus, the imaginary component. The amplitude test for various compositions of the hydrogels at 1 Hz represented the outcome of G' and G'' vs shear strain (%) in Figures 2 (b, c) which demonstrate that with increasing the percentage of CMC into the alginate suspension, the physical state of the hydrogel is approaching from liquid-like to solid-like state. The liquid-like state was persisted for all compositions due to domination of the loss modulus over the storage modulus in all compositions. Loss tangent ($tan\delta = G''/G'$) value smaller than 1 predominantly reflects the elastic behavior, and greater than 1 predominantly indicates viscous behavior. Figures 2 (b, c) indicate that the difference between G'' and G' was reduced with increasing the weight percentage of CMC in the composition. The $tan\delta$ value increased with increasing the shear strain, which indicates the dominance of liquid-like state over solid-state. Therefore, we can conclude that with less shear strain, G' may dominant which will help to maintain the shape fidelity of the fabricated scaffold with compositions having more content weight of CMC. Fabricating cell encapsulated scaffolds with less applied pressure will also minimize the cell death in post-printing period and eventually will increase cell viability in long incubation period [28].

3.3. Hydrogel recovery rate

To determine the recovery rate after extrusion, a three point-interval-thixotropy-test was conducted on all the compositions which is directly related to the shape fidelity of the filament. The first interval of the test imitates the at-rest state of sample, the second interval resembles the hydrogel decomposition under high shear, and third interval reflects the structure retention after hydrogel extrusion as shown in Figure 3(a).

A shear rate of $1.0 \, s^{-1}$ was applied for 60 seconds at first. Then, the shear rate was increased to $100 \, s^{-1}$ for 5 seconds. Finally, shear rate was reduced to $1.0 \, s^{-1}$ and held for $120 \, seconds$. Figure 3(a) shows that the recovery rate of A_2C_6 was 87% of its viscosity after 60 seconds where the recovery rate increased to 90% after 120 seconds. Therefore, it is a good indication that the deposited filament will hold the shape to maintain the geometric fidelity. The recovery rates of A_0C_8 , A_4C_4 , A_6C_2 , and A_0C_8 after 60s and 120s are shown in Figure 3(b). Even though A_6C_2 and A_0C_8 were showing very promising recovery rate, there is a high chance these combinations will demonstrate over-deposition and eventually poor shape fidelity due to lower initial viscosity than other considered compositions. In terms of recovery rate and initial viscosity, A_2C_6 and A_4C_4 can be good candidates for 3D bio-printing.

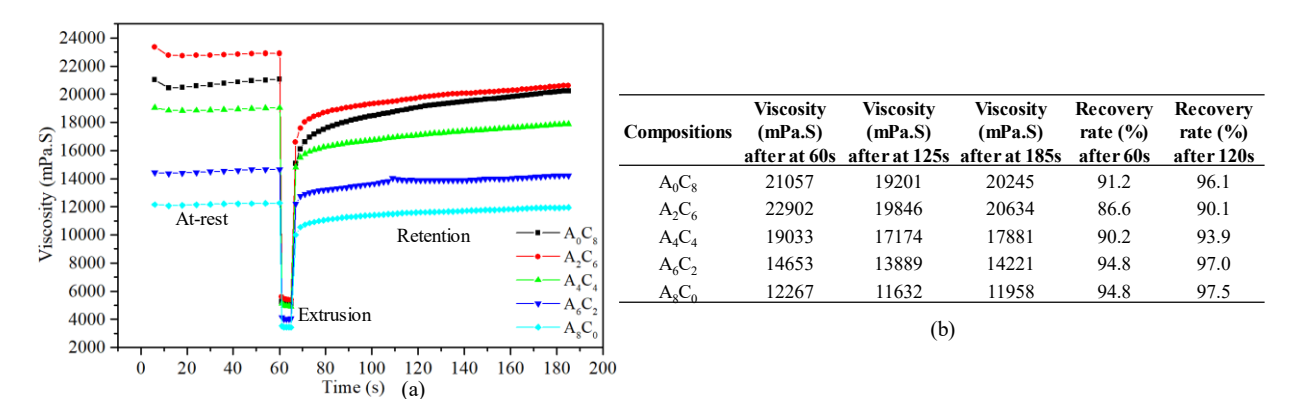


Figure 3: (a) Three-point thixotropic test and (b) Recovery rate of various compositions at 60s and 120s.

4. 3D scaffold fabrication

BioX (CELLINK, Boston, MA), a three-axis 3D bioprinter, is used to fabricate the scaffold. A set of 3D scaffolds were fabricated by extruding all compositions pneumatically on a stationary build plane. The printing parameters we used to fabricate the scaffolds were a nozzle diameter of 410 μm, print speed of 10 mm/s, air pressure of 50 kPa, and print distance of 0.405mm. A Computer-Aided Design (CAD) software called Rhino 6.0 (https://www.rhino3d.com) was used to design and define the vectorized toolpath of a scaffold. A G-code generator software named Slicer (https://www.slicer.org) was used to generate a Bio-X compatible file including the toolpath coordinates and all process parameters to fabricate the scaffold. A layer-upon-layer fashion was followed to deposit materials. As a physical crosslinked, 4% (w/v) CaCl₂ was used after the scaffold fabrication. An overview of scaffold fabrication process is schematically shown in Figure 4.

Filaments without encapsulating any cell i.e. acellular were deposited with the compositions of A0C8, A2C6, A4C4, A6C2, and A8C0 for investigating their printability. The images of fabricated filaments are captured using the CK Olympus bright field microscope (Tokyo, Japan). The width of the filament is determined using ImageJ. Fabricated scaffolds and corresponding filaments with their width are shown Figure 5. This figure indicates that with increasing the solid content of CMC into the composition, the diffusion of the filament decreased, i.e. properly holding the geometry of the filament, which eventually will improve the overall shape fidelity of the fabricated scaffold.

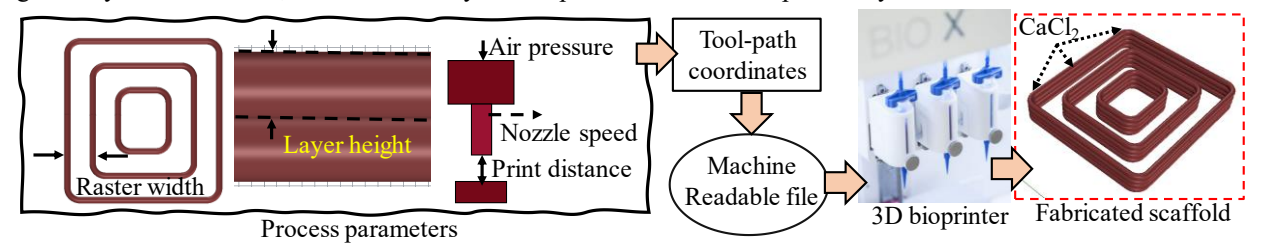


Figure 4: Preparing machine-readable file and execution of 3D fabrication.

Filament fabricated with the composition of A_2C_6 showed better shape holding ability. Filaments fabricated with A_0C_8 , A_4C_4 , A_6C_2 , and A_8C_0 showed 17%, 48%, 77% and 94% more diffusion than filament fabricated with A_2C_6 . Figure 5(a) also represents the crosslinked scaffolds and filaments. Scaffold fabricated with A_0C_8 composition almost dissolved into $CaCl_2$ due to the absence of alginate.

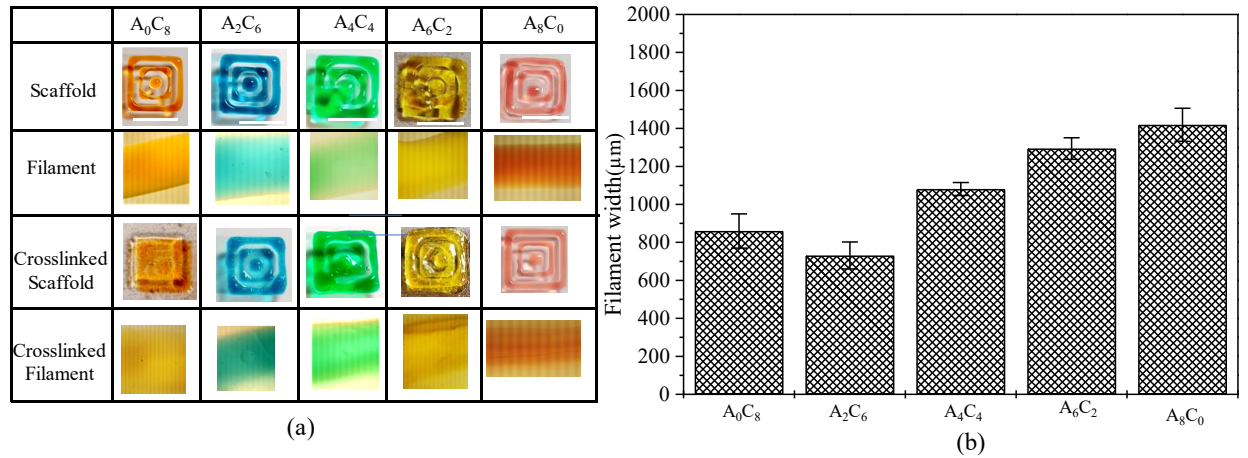


Figure 5: (a) Scaffolds and filaments fabricated with various compositions and (b) Filament width.

5. Discussion

Various efforts have been reported to prepare hybrid hydrogels to achieve the proper rheological properties to help print the scaffolds to maintain the shape fidelity [29]. In our earlier work, we used high viscous CMC into alginate to analyze printability, shape fidelity and cell viability [22]. To our best knowledge, the effect of low viscous CMC on bio-printing process is not reported. In this paper, a hybrid hydrogel was prepared mixing carboxymethyl cellulose (lower molecular weight) with low viscosity at different weight percentages with alginate with an overall 8% (w/v) total solid content. A₂C₆ shows highest viscosity (37633 cps) which is within the limit of 300-100000 cps as shown in Figure 2. Various rheological tests were conducted to determine the effect of low viscous CMC on the hybrid hydrogels in term of viscosity, shear stress, storage modulus, loss modulus, and recovery rate. The relationship between the printability and rheological properties of the compositions were identified. Results showed compositions A₂C₆ and A₄C₄ having higher viscosity at lower shear rate and higher post-printing recovery rate can create filament with proper shape fidelity. Since, hydrogel with lower viscosity can better assist the cell proliferation [18], we can expect that this composition will show better cell viability in incubation period. Therefore, the future direction of this research is to identify the maximum height of the scaffolds, A₂C and A₄C₄ compositions can fabricate ensuring shape fidelity. Moreover, the scaffolds will be fabricated with A₂C₆ and A₄C₄ compositions encapsulating cell and analyzed the cell viability and proliferation.

6. Conclusion

This research identified a rheological analysis of various compositions prepared with alginate and low viscous CMC maintaining a solid content of 8%. The effect of low viscous CMC on the hybrid hydrogels was determined in terms of viscosity, shear stress, storage modulus, loss modulus, and recovery rate. The relationship between the printability and rheological properties of the compositions were demonstrated. The illustrated rheological tests and corresponding printability of those compositions can direct the 3D bio-fabrication of the tailored anisotropic scaffolds, which will assist in future efforts to fabricate functional tissues.

Acknowledgements

Research was supported by New Hampshire-EPSCoR through BioMade Award #1757371 from National Science Foundation and New Hampshire-INBRE through an Institutional Development Award (IDeA), P20GM103506, from the National Institute of General Medical Sciences of the NIH.

References

- Murphy, S.V. and A. Atala, 3D bioprinting of tissues and organs. Nature biotechnology, 2014. 32(8): p. 773-785
- 2. Jia, W., et al., *Direct 3D bioprinting of perfusable vascular constructs using a blend bioink.* Biomaterials, 2016. **106**: p. 58-68.
- 3. Wang, L.L., et al., 3D extrusion bioprinting of single-and double-network hydrogels containing dynamic covalent crosslinks. Journal of Biomedical Materials Research Part A, 2018.

- 4. Malda, J., et al., 25th anniversary article: engineering hydrogels for biofabrication. Advanced materials, 2013. 25(36): p. 5011-5028.
- 5. M'barki, A., L. Bocquet, and A. Stevenson, *Linking Rheology and Printability for Dense and Strong Ceramics by Direct Ink Writing*. Scientific Reports, 2017. 7(1): p. 6017.
- 6. Ahlfeld, T., et al., A methylcellulose hydrogel as support for 3D plotting of complex shaped calcium phosphate scaffolds. Gels, 2018. 4(3): p. 68.
- 7. Jin, Y., et al., Self-Supporting Nanoclay as Internal Scaffold Material for Direct Printing of Soft Hydrogel Composite Structures in Air. ACS Applied Materials & Interfaces, 2017. 9(20): p. 17456-17465.
- 8. Di Giuseppe, M., et al., *Mechanical behaviour of alginate-gelatin hydrogels for 3D bioprinting*. Journal of the mechanical behavior of biomedical materials, 2018. **79**: p. 150-157.
- 9. Tabriz, A.G., et al., *Three-dimensional bioprinting of complex cell laden alginate hydrogel structures*. Biofabrication, 2015. **7**(4): p. 045012.
- 10. Kuo, C., et al., *Printability of Hydrogel Composites Using Extrusion-Based 3D Printing and Post-Processing with Calcium Chloride.* J Food Sci Nutr, 2019. **5**: p. 051.
- 11. Kiyotake, E.A., et al., *Development and quantitative characterization of the precursor rheology of hyaluronic acid hydrogels for bioprinting.* Acta biomaterialia, 2019.
- 12. Kirchmajer, D.M. and R. Gorkin Iii, *An overview of the suitability of hydrogel-forming polymers for extrusion-based 3D-printing*. Journal of Materials Chemistry B, 2015. **3**(20): p. 4105-4117.
- 13. Chen, Y., et al., 3D Bioprinting of shear-thinning hybrid bioinks with excellent bioactivity derived from gellan/alginate and thixotropic magnesium phosphate-based gels. Journal of Materials Chemistry B, 2020.
- 14. Colosi, C., et al., *Microfluidic Bioprinting of Heterogeneous 3D Tissue Constructs Using Low-Viscosity Bioink.* Advanced Materials, 2016. **28**(4): p. 677-684.
- 15. Therriault, D., S.R. White, and J.A. Lewis, *Rheological behavior of fugitive organic inks for direct-write assembly.* Applied Rheology, 2007. **17**(1): p. 10112-11411.
- 16. Ouyang, L., et al., Effect of bioink properties on printability and cell viability for 3D bioplotting of embryonic stem cells. Biofabrication, 2016. **8**(3): p. 035020.
- 17. He, Y., et al., Research on the printability of hydrogels in 3D bioprinting. Scientific reports, 2016. **6**: p. 29977.
- 18. Khalil, S. and W. Sun, *Bioprinting endothelial cells with alginate for 3D tissue constructs*. Journal of biomechanical engineering, 2009. **131**(11): p. 111002.
- 19. Göhl, J., et al., Simulations of 3D bioprinting: predicting bioprintability of nanofibrillar inks. Biofabrication, 2018. **10**(3): p. 034105.
- 20. Gao, T., et al., *Optimization of gelatin–alginate composite bioink printability using rheological parameters:* a systematic approach. Biofabrication, 2018. **10**(3): p. 034106.
- 21. Jiang, Y., et al., *Rheological behavior, 3D printability and the formation of scaffolds with cellulose nanocrystals/gelatin hydrogels.* Journal of Materials Science, 2020. **55**(33): p. 15709-15725.
- 22. Habib, A., et al., 3D printability of alginate-carboxymethyl cellulose hydrogel. Materials, 2018. 11(3): p. 454.
- 23. Garrett, Q., et al., Carboxymethylcellulose binds to human corneal epithelial cells and is a modulator of corneal epithelial wound healing. Investigative ophthalmology & visual science, 2007. **48**(4): p. 1559-1567.
- 24. Kim, M.S., et al., *Ionically crosslinked alginate–carboxymethyl cellulose beads for the delivery of protein therapeutics*. Applied Surface Science, 2012. **262**: p. 28-33.
- 25. Han, Y. and L. Wang, *Sodium alginate/carboxymethyl cellulose films containing pyrogallic acid: physical and antibacterial properties.* Journal of the Science of Food and Agriculture, 2017. **97**(4): p. 1295-1301.
- 26. Tongdeesoontorn, W., et al., Effect of carboxymethyl cellulose concentration on physical properties of biodegradable cassava starch-based films. Chemistry Central Journal, 2011. 5(1): p. 6.
- 27. Li, H., et al., 3D bioprinting of highly thixotropic alginate/methylcellulose hydrogel with strong interface bonding. ACS applied materials & interfaces, 2017. 9(23): p. 20086-20097.
- 28. Chang, R., J. Nam, and W. Sun, *Effects of dispensing pressure and nozzle diameter on cell survival from solid freeform fabrication—based direct cell writing.* Tissue Engineering Part A, 2008. **14**(1): p. 41-48.
- 29. Ahlfeld, T., et al., Development of a clay based bioink for 3D cell printing for skeletal application. Biofabrication, 2017. 9(3): p. 034103.